Progress in Nuclear Magnetic Resonance Spectroscopy 94-95 (2016) 1–10

Contents lists available at ScienceDirect

Progress in Nuclear Magnetic Resonance Spectroscopy

journal homepage: www.elsevier.com/locate/pnmrs

Diffusion NMR studies of macromolecular complex formation, crowding and confinement in soft materials

Suliman Barhoum, Swomitra Palit, Anand Yethiraj *

Department of Physics and Physical Oceanography, Memorial University, St. John's, Newfoundland and Labrador, Canada

Edited by Gareth Morris and David Neuhaus

ARTICLE INFO

Article history:
Received 18 December 2015
Accepted 28 January 2016
Available online 4 February 2016

Keywords:
Pulsed-field gradient NMR
Complex formation
Crowding
Confinement
Soft materials

ABSTRACT

Label-free methods to obtain hydrodynamic size from diffusion measurements are desirable in environments that contain multiple macromolecular species at a high total concentration: one example is the crowded cellular environment. In complex, multi-species macromolecular environments – in this article, we feature aqueous systems involving polymers, surfactants and proteins – the link between dynamics and size is harder to unpack due to macromolecular crowding and confinement. In this review, we demonstrate that the pulsed-field gradient NMR technique, with its spectral separation of different chemical components, is ideal for studying the dynamics of the entire system simultaneously and without labelling, in a wide range of systems. The simultaneous measurement of the dynamics of multiple components allows for internal consistency checks and enables quantitative statements about the link between macromolecular dynamics, size, complex formation and crowding in soft materials.

Contents

1. Introduction

Biological cells contain high concentrations of macromolecules, such as proteins, nucleic acids, actin filaments, cytoskeletons, and organelles that occupy a significant part (between 7% and 40%) of the total volume [1–3]. Such "macromolecular crowding" is believed to play an important role in diffusive transport inside the cell [4–11]. Macromolecules in a crowded biological cell interact via various specific and non-specific interactions [12]. Often there are many competing interactions of similar strength, presenting a challenge for a comprehensive understanding of intracellular transport. Our approach is to build simple model systems with increasing levels of complexity in order to capture, in a recursive manner, the details and complexities of real biological systems.

Transport properties of macromolecules are commonly studied in vitro by constructing cell-mimetic environments. This has been accomplished by adding high concentrations of inert, uncharged crowding agents such as polyethylene glycol (PEG), charged crowding agents such as bovine serum albumin (BSA) [6], globular

* Corresponding author.

http://dx.doi.org/10.1016/j.pnmrs.2016.01.004
0079-6565/

proteins such as lysozyme [13], and polysaccharides such as dextran and Ficoll [14–16] to the solution. The study of such multicomponent macromolecular solutions can provide quantitative answers for important open questions: When do crowding effects become significantly important? What is the average size of the macromolecular aggregates? What is the composition of these multi-component aggregates? What is the role of electrostatics?

While the intent of this review is to showcase the power of magnetic-resonance-based techniques to address these questions, we begin by briefly reviewing other established experimental methodologies. There are two commonly used methods to obtain macromolecular sizes: *via* dynamics, dynamic light scattering, and *via* structure, small-angle (X-ray or neutron) scattering. The most convenient, and thus most common, is the dynamics-based method, dynamic light scattering (DLS). All dynamics-based methods measure macromolecular diffusion coefficients and use it to obtain the hydrodynamic radius (R_H), which is usually defined *via* the Stokes–Einstein–Sutherland equation,

$$D_0 = \frac{k_B T}{6\pi\eta R_H}, \tag{1}$$

where k_B is the Boltzmann constant, T is the temperature, η is the viscosity of the solvent and D_0 is the measured diffusion coefficient. The Stokes–Einstein–Sutherland equation is only valid for solutes at infinite dilution; at finite concentrations there are hydrodynamic interactions between diffusing species. Different models have been proposed to approximate the interactions of hard spheres [17,18] and charged spheres [19,20] as a function of the particle volume fraction ϕ; the hydrodynamic interaction only gets more complicated for interacting particles with more complex shapes.

In DLS, fluctuations in the intensity of scattered light occur due to the Brownian motions of macromolecules in solution. Smaller macromolecules that diffuse more quickly give rise to more rapid fluctuations; the intensity autocorrelation function contains all the information regarding the diffusion of macromolecules within the sample being measured [21]. For a single species, the diffusion coefficient (D_0) is obtained by fitting the autocorrelation function to an exponential function, with D_0 being proportional to the lifetime of the exponential decay. Among the techniques used to study macromolecular systems, dynamic light scattering has proved to be one of the most useful since it allows measurements to be made of both the spatial and the temporal correlation between the macromolecules. It, however, has an inherent limitation: in studies of multi-component systems, the scattered light intensity has information from all the particle species simultaneously. Fluorescence correlation spectroscopy (FCS), which measures self-diffusion of fluorescent-labelled macromolecules, is an alternative method to get around this challenge.

A direct structure-based method for obtaining macromolecular size is the small-angle scattering technique, which includes small-angle neutron scattering (SANS) and small-angle X-ray scattering (SAXS). These techniques are based on the interaction occurring between the incident radiations (neutrons, X-rays) and the particles present in the system under investigation. Unlike DLS, which measures fluctuations in scattering, these techniques measure static (i.e. time-averaged) scattering curves. The fact that X-rays and neutrons have much shorter wavelengths than does visible light makes analysis of such static scattering measurements a useful approach for characterizing macromolecular sizes and shapes. In a SANS experiment, for example, the neutron beam is scattered by the sample and the intensity of the scattered beam at the scattering angle θ is measured. Scattering data are usually presented as plots of the intensity of the scattered neutron beam, $I(q)$, versus the scattering vector (q) which is proportional to θ. The intensity can be written as $I(q) = I_0 P(q)$, where $P(q)$, known as the form factor, provides information on the size and shape of the scatterers. In the limit of very low angle or small q (the Guinier approximation) one can further write

$$I(q) = I_0 \exp\left(\frac{-q^2 R_g^2}{3}\right), \tag{2}$$

where the radius of gyration of the scattering object, R_g, can be extracted from the slope of a plot of $\ln(I/I_0)$ vs q^2. However, in order to study a system consisting of multiple species of macromolecules via small angle scattering one needs species-selective contrast matching [22]. For neutron scattering this relies on the different scattering lengths of hydrogen and deuterium. This means that molecules containing hydrogen may have their scattering length density varied by replacement with deuterium. The scattering length density of H_2O is negative, and that of D_2O is positive. The proportions of H_2O and D_2O have to be adjusted such that particular macromolecules are contrast-matched, so that they effectively become transparent to neutrons.

Pulsed-field gradient (PFG) NMR is a powerful dynamics-based measurement technique that can provide a quantitative measure of molecular motion over the millisecond to second time scale [23]. While it cannot probe the short (microsecond) timescales probed by DLS, chemical shift provides an avenue for tracking multiple chemical species simultaneously. This is now routine in small-molecule "diffusion-ordered spectroscopy", or DOSY, experiments [24,25]. The Stokes–Einstein–Sutherland relation (Eq. (1)), which is only truly valid at infinite dilution, may then used to obtain the hydrodynamic radius of each chemical species from the respective diffusion coefficient D_0. PFG-NMR has also emerged as an important tool to measure self-diffusion in complex fluids [26,27] such as macromolecular (surfactant and polymer) systems [28]. For complex fluids, the relation between hydrodynamic size and diffusion coefficient is more complicated. The diffusing species in complex fluids are often interacting with neighbouring macromolecules *via* the hydrodynamic interaction, and the diffusion coefficient may be written as

$$D(\phi) = h(\phi) D_0, \tag{3}$$

where $h(\phi)$ is the "hydrodynamic function" that is determined by hydrodynamic interactions at non-zero macromolecular volume fraction ϕ. Except in the simplest of cases (e.g. hard spheres [17]), the hydrodynamic function is difficult to obtain, and therefore it is valuable to be able to measure $h(\phi)$ experimentally in multicomponent systems.

In this review, we present recent developments in NMR studies of diffusion in complex-forming systems, primarily using extracts from our own work as examples, and focusing on the interpretation of data from PFG-NMR experiments. We point the reader to earlier (and excellent) reviews [26,27] for the PFG-NMR technique fundamentals.

The ^{1}H nucleus is most suitable for PFG-NMR measurements because of its high gyromagnetic ratio. Polymer chains, for example, have a high content of ^{1}H ideally suited for PFG-NMR experiments. In polymer–surfactant solutions, the surfactants are found in monomeric, aggregate, and micellar form. A simple self-consistent model has been introduced effectively to quantify the variation of the free monomer concentration and free micellar concentration over the entire range of surfactant concentration [29]. In addition, we explore the validity of a similar mathematical model for complex formation in peptide–micelle systems [30]. In brief, the article showcases the richness of the information that can be obtained using NMR diffusometry in concert with simple models of macromolecular association.

In Section 3, we present PFG-NMR measurements that were utilized to investigate polymer–surfactant solutions at varying

concentrations [29]. We introduce a self-consistent model that takes into account the fact that the surfactants are found in monomeric, aggregate, and micellar form. We use experimental data and a simple model to quantify the variation of the free monomer concentration and free micellar concentration over the entire range of surfactant concentration.

In Section 4, we discuss the crucial question of data analysis in PFG-NMR. In cluster-forming systems, the residence time of a macromolecule within an aggregate is inversely dependent on the critical aggregation concentration, and thus the characteristic time for each system is different; this timescale determines how one should interpret the diffusion measurements in cluster-forming systems.

In Section 5, we explore complex formation in peptide–micelle systems [30], where NMR diffusion measurements were used to study the interaction between the cationic GAD-2 antimicrobial peptide (AMP) and an anionic SDS micelle used as a membrane mimic environment. A mathematical model similar to the one used in the polymer–surfactant study (Section 3) was employed in order to make quantitative statements about the limitations inherent to obtaining the hydrodynamic size of macromolecular complexes.

Finally, in Section 6, we examine a surfactant mixture that forms long, cylindrical wormlike aggregates. Here, the surfactant molecule has a much longer residence time within an aggregate, and one therefore sees molecular diffusion within an aggregate coupled with aggregate diffusion.

2. Experimental methods

Five types of macromolecules are used as examples for this review. A non-ionic polymer polyethylene oxide (PEO, with formula mass 20,000), an anionic surfactant sodium dodecylsulphate (SDS, with average molecular mass of 288.38), a roughly spherical polysacchharide ("Ficoll-70", with average molecular mass 70 kDa), an anti-microbial peptide ("GAD-2", with average molecular mass of 2168), and a zwitterionic surfactant, N-tetradecyl-N, N-dimethyl-3-ammonio-1-propanesulfonate (TDPS, $M_w = 363.6$). All NMR-based experiments reported here (except those in Fig. 6) were conducted at a resonance frequency of 600 MHz on a Bruker Avance II spectrometer and at sample temperature 298 K. The diffusometry measurements were carried out on diffusion probe (Diff 30) with maximum field gradient of 1800 G/cm, using a pulsed-field gradient stimulated-echo sequence [31] (see Fig. 1). The diffusion coefficients for the molecular components in aqueous solution were obtained from the attenuation of the signals. An example, shown in Fig. 2(a), is the 1D proton NMR spectrum for a PEO

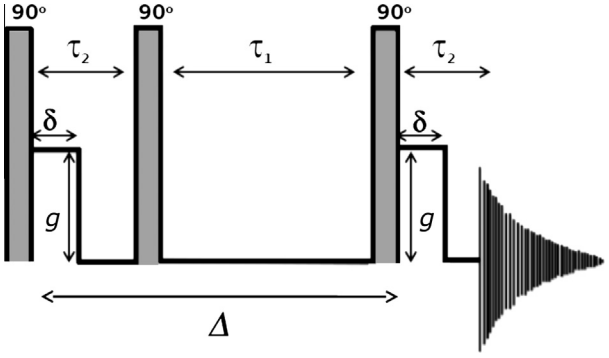

Fig. 1. The pulsed-field gradient stimulated echo pulse sequence. Longitudinal relaxation occurs during the time τ_1, transverse relaxation during the time τ_2, and Δ is the diffusion time. The gradient pulses are of amplitude g and duration δ, and applied after the first and third 90° rf pulse (the rf pulses are shaded grey). A typical experiment had the parameters $\tau_2 \sim 3$ ms, $\tau_1 = 97$ ms, $\delta = 2$ ms, and $\Delta = 100$ ms.

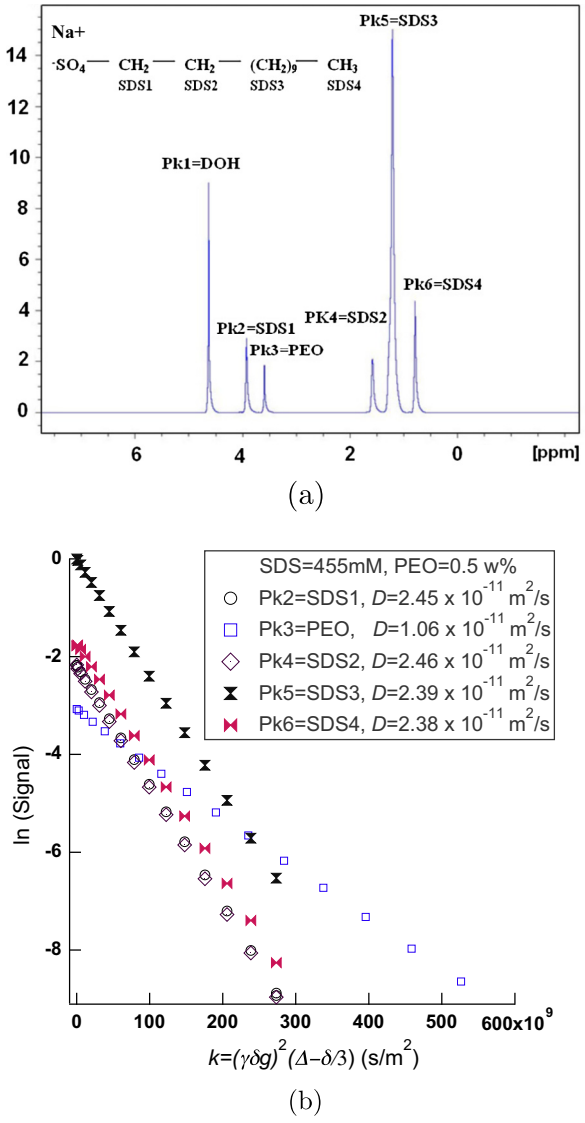

Fig. 2. (a) 1D ^{1}H NMR spectrum for a PEO (0.5% w/v)/ SDS (455 mM)/D_2O sample at a sample temperature of 298 K. Inset: the chemical formula of SDS. (b) The attenuation of the signal $S(k)/S(0)$ on a log scale versus $k = (\gamma\delta g)^2(\Delta - \delta/3)$ for PEO(0.5%w/v)/SDS (455 mM)/D_2O sample with $\delta = 2 \times 10^{-3}$ s, $\Delta = 100 \times 10^{-3}$ s. Reproduced with permission from S. Barhoum and A. Yethiraj, J. Chem. Phys. 2010, 132, 024909. Copyright 2010, AIP Publishing LLC.

(0.5%w/v)/SDS (455 mM)/D_2O sample. The spectrum shows six spectrally separated peaks, labelled as peak 1 (HDO), created due to the quick exchange of protons between D_2O and H_2O molecules in the solution, peaks 2 and 4–6, associated with the protons of the SDS molecule (i.e. SDS1, SDS2, SDS3, SDS4) as in the inset of Fig. 2 (a), and peak 3, associated with the protons of the PEO molecule. The signal attenuation (Fig. 2(b)), associated with different molecular components was obtained based on the location of the labelled peaks in the 1D proton NMR spectrum. The diffusion coefficients of different components were obtained from an exponential fit of the signal attenuation [31] which exhibits monoexponential behaviour for the three components over the entire range of SDS concentration. The signal attenuation was fitted to the form

$$S(k) = S(0)\exp(-Dk), \tag{4}$$

where $S(k)$ is the intensity of the signal in the presence of field gradient pulse, $S(0)$ is the intensity of the signal in the absence of field gradient pulse, $k = (\gamma g \delta \Delta)^2(\Delta - \delta/3)$, $\gamma = \gamma^H = 2.657 \times 10^8$ T^{-1} s^{-1} is

the proton gyromagnetic ratio, $\delta = 2$ ms is the duration of field gradient pulse, $\Delta = 100$ ms is the time period separating the mid-point of the two field gradient pulses, and g is the amplitude of field gradient pulse. Each peak in Fig. 2(a) yields an independent diffusion coefficient, shown in the legend (errors are in the third decimal place in all cases). In the PEO-SDS system, the signal attenuations of the different chemical species always exhibit this mono-exponential dependence. Situations where this is not the case are discussed in Section 4.

3. Aggregate formation in a polymer–surfactant system

The aqueous solution of a nonionic polymer poly(ethylene oxide) (PEO) and an anionic surfactant sodium dodecylsulphate (SDS) is a simple model for studying macromolecular complex formation. The PEO-SDS system has been investigated using different techniques such as NMR diffusometry [32,33], NMR relaxometry [33,34], viscosity [32,35], and conductivity measurements [35–37]. These studies found different concentration regimes, bounded by distinct concentrations: the critical aggregation concentration (CAC) at which SDS anions start associating with PEO chains, the SDS concentration C_2 at which PEO chains are saturated, and the SDS concentration at which SDS micelles exhibit spherical to cylindrical transition. NMR diffusometry and electrophoretic NMR studies on the interaction between polymer and surfactants in PEO-SDS system reported that each surfactant/polymer complex contains micelles adsorbed on the PEO chain for a surfactant concentration regime higher than the CAC [38]. This is consistent with earlier findings on this very system [39,40]. The nature of micelle formation was also studied in the binary system SDS/water using NMR relaxometry [34] to identify the CMC (i.e. critical micellar concentration) at which surfactants start forming micelles.

Barhoum and Yethiraj [29] used NMR diffusometry to detect the onset of macromolecular crowding. In their work, diffusion measurements were carried out on surfactant solutions with and without polymer. For PEO-free SDS in buffered and unbuffered systems, Fig. 3(a) shows that the variation of the observed SDS diffusion coefficient D^{SDS}_{Obs} with concentration shows a plateau at low SDS concentration that is followed by a rapid decrease at concentrations above the critical micellar concentration (CMC). Hence, in the SDS concentration regime below CMC, the SDS is in the monomeric state while in the SDS concentration regime above CMC, the SDS is partitioned between monomeric and micellar states. The fact that the signal attenuation associated with the SDS peak exhibits monoexponential behaviour (Fig. 2(b)) over the whole range of SDS concentration suggests that the exchange between SDS micelles and free solution must be very rapid on the NMR time scale. Therefore, for the pure (PEO-free) SDS system, the observed self-diffusion coefficient of SDS is a linear combination of the self-diffusion coefficient D^{SDS}_{free} of the free molecules in bulk and that of the bound molecules in the micelle $D^{SDS}_{micelle}$ or aggregate D^{SDS}_{Aggr} in PEO-free SDS and PEO-SDS solutions respectively. The validity of this "two-species model" has long been known [41–43]. Using the two-species model, the diffusion coefficient is written as:

$$D^{SDS}_{Obs} = D^{SDS}_{free}, \quad C^{SDS} \leqslant C_0,$$
$$D^{SDS}_{Obs} = \left(D^{SDS}_{free} - D^{SDS}_{Aggr}\right) f_s + D^{SDS}_{Aggr}, \quad C^{SDS} > C_0 \qquad (5)$$

where $f_s = C^{SDS}_{free} / C^{SDS}$ is the fraction of free SDS molecules, D^{SDS}_{Aggr} is either the micellar diffusion coefficient $D^{SDS}_{micelle}$ in PEO-free samples, or the diffusion coefficient of the surfactant–polymer aggregate in the PEO-SDS system, C_0 is the critical (micellar or aggregation) concentration (CMC or CAC), and C^{SDS} is the total SDS concentration.

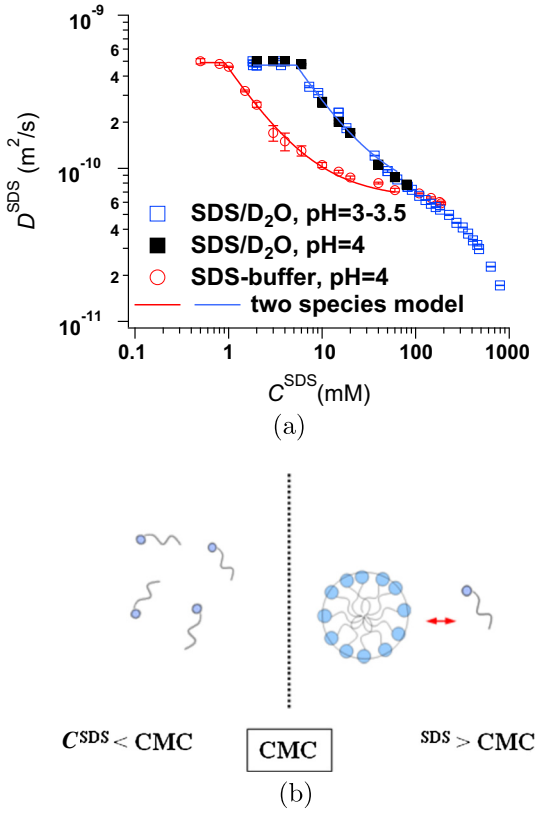

Fig. 3. (a) SDS self-diffusion coefficient in SDS/D_2O versus SDS concentration C^{SDS} for solutions with sodium oxalate buffer (pH = 4) (red open circles), and unbuffered, with pH = 3–3.5 (blue open squares), and with pH = 4 (black filled squares). (b) Schematic diagram for the partitioning of SDS in the SDS/D_2O system: monomers for C^{SDS} < CMC, and micelles and monomers for CMC < C^{SDS}. Reproduced with permission from S. Barhoum and A. Yethiraj, J. Chem. Phys. 2010, 132, 024909. Copyright 2010, AIP Publishing LLC.

The observed diffusion coefficient D^{SDS}_{Obs} in Fig. 3(a) for buffered ($pH = 4$) and unbuffered ($pH = 3$—3.5) SDS solutions [30] is fitted to the piece-wise function in Eq. (5). Thus at low SDS concentrations, one can determine the CMC, which for ionic surfactants is very sensitive to the electrostatic environment, very precisely.

We also see, in Fig. 3(a), that the fit to a two-species model is no longer possible above $C^{SDS} = 60$ mM, and that there is a convergence of the dynamics of SDS in different electrostatic environments. This indicates that systems enter into a regime where intermicellar hydrodynamic interactions dominate the behaviour and mask the effect of differences in aggregate size and of small differences in the net charge. Such an effect of hydrodynamic interactions has indeed been previously noted [44] and, in macromolecular systems, is broadly termed "crowding".

The diffusion coefficient of polymer (PEO), surfactant (SDS) and HDO in unbuffered PEO(0.5%w/v)/SDS/D_2O, shown in Fig. 4(a), was obtained for the whole range of SDS concentration. These results allow a self-consistent assessment of the range of validity of the two-species model (Eq. (5)). Assuming $D^{SDS}_{Aggr} = D^{PEO}_{Obs}$, one may calculate the "free" fraction of SDS (f_s) in monomeric state (Fig. 4(b), inset) as well as the concentration ($C^{SDS}_{free} = f_s C^{SDS}$, in mM) of the same over the entire range of SDS concentration (Fig. 4(b)).

In the range between 3.5 mM and 60 mM, C^{SDS}_{free} stays constant. In simple models of surfactant self-assembly (see, for example, [45] or [46]), a plot of monomer versus the total concentration has slopes of 1 and 0, respectively, below and above the CAC. Above

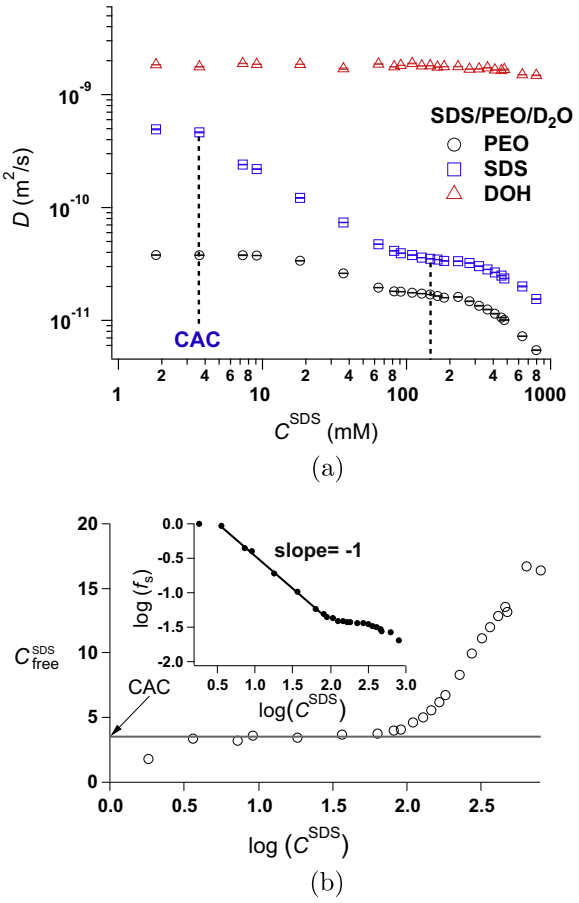

Fig. 4. (a) Self-diffusion coefficient of polymer (PEO), surfactant (SDS) and HDO in PEO (0.5% w/v)/SDS/D_2O vs SDS concentration. (b) A fit to the two-species model (Eq. (5)) yields the fraction of free surfactant (inset) as a function of the total surfactant concentration in solution. The concentration of free surfactant C_{free}^{SDS} stays constant when the total surfactant exceeds the CAC. The apparent rise at large C^{SDS} signals the breakdown of the two-species model. Reproduced with permission from S. Barhoum and A. Yethiraj, J. Chem. Phys. 2010, 132, 024909. Copyright 2010, AIP Publishing LLC.

the CAC, the concentration of free surfactant should stay constant, with a monomer concentration that equals the CAC, because all additional surfactant is going to forming new micelles. The plateau in C_{free}^{SDS} is thus a very sensitive measure of the CAC. To our knowledge, PFG-NMR appears to be the only method that provides such a direct measurement of the monomer concentration.

On the other hand, we have to consider the rise in C_{free}^{SDS} in the context of what we saw for the pure surfactant in Fig. 3(a), where the observed diffusion coefficient cannot be fitted to a two-species model above ~60 mM. We may thus identify this as the onset of crowding in the SDS-PEO system. Essentially, beyond this point, we cannot use observed diffusion coefficients to obtain information about the composition of the system. We will revisit this point again, in the context of peptide–surfactant complexes, in Section 5.

4. Interpretive diffusion models and their validity

In the last section, we introduced the study of aggregation in a polymer–surfactant system. It is worthwhile to summarize the assumptions underlying Eq. (5). First, the echo signal from each of the peaks in the ^1H spectrum of the PEO-SDS system shows a monoexponential decay with the gradient strength parameter $k(t)$ which is a function of the diffusion time $t = \Delta$ (Fig. 2(b)). For example, all the SDS peaks show a monoexponential decay. This implies either that the peaks report on a single component (e.g. SDS monomer) or that, if there are multiple components (e.g. a monomer and an SDS-containing aggregate), SDS exchanges very rapidly between monomer and aggregate on the timescale of milliseconds corresponding to that of the chemical shift.

The residence time of the surfactant molecule τ_R within an aggregate is given [45] by the diffusion time τ_0 (which is on the nanosecond scale) and the CMC (in molar units):

$$\tau_R \sim 55\tau_0/\mathrm{CMC}. \tag{6}$$

For aggregation concentrations in the mM range, the residence times are on the microsecond scale. Exchange of SDS between monomer and aggregate is thus reasonably rapid, and one can consider the mean-square displacement of a single molecule (along the z axis) in time t to be governed by the fraction of time spent in monomer (f) and aggregate ($1-f$) environments:

$$\langle z^2(t)\rangle = 2fD_{\mathrm{monomer}}t + 2(1-f)D_{\mathrm{aggregate}}t \equiv 2D_{\mathrm{Obs}}t \tag{7}$$

with $D_{\mathrm{Obs}} = fD_{\mathrm{monomer}} + (1-f)D_{\mathrm{aggregate}}$, thus agreeing with Eq. (5).

On the other hand, in systems where the CMC is very low (e.g. lipids) or where τ_0 is larger (e.g. 100 nm to 1 μm scale colloids), Eq. (6) predicts long residence times; this results in slow exchange between monomer and aggregate. Here, one expects the total signal to be given by

$$\begin{aligned} S_{\mathrm{total}} &= S_{\mathrm{monomer}} + S_{\mathrm{aggregate}} \\ &= S_{0,\mathrm{monomer}}\exp(-D_{\mathrm{monomer}}k) + S_{0,\mathrm{aggregate}}\exp(-D_{\mathrm{aggregate}}k) \end{aligned} \tag{8}$$

which is bi-exponential in nature. The relevant duration $t = \Delta$ in the PFG-NMR experiment is linearly related to the gradient parameter, $k(\Delta) = (\gamma\delta g)^2(\Delta - \delta/3)$. A generalization to multi-exponential behaviour may be made for more than two species of macromolecules: $S_{\mathrm{total}} = \sum_i S_i \exp(-D_i k)$. For two species, Eq. (8) may be written in the form

$$S_{\mathrm{total}}/S_{\max} = f\exp(-D_1 k(t)) + (1-f)\exp(-D_2 k(t)), \tag{9}$$

where $f = S_1/(S_1+S_2)$ (and we have dropped the subscript "0"). When the arguments to the diffusion exponentials are small, the exponentials may be expanded, summed and then re-written as an exponential to yield Eq. (5).

Examples of both mono- and biexponential behaviour are seen in a classic polysaccharide crowder (Ficoll-70): given the larger size, the diffusion time of the monomer $\tau_0 \sim 1$ μs; thus residence times τ_R in clusters will be a few microseconds or longer. Like any single species system, the PFG-NMR signal attenuation of Ficoll-70 is monoexponential at low concentration (Fig. 5(a)), but at high concentration a fraction of Ficoll forms aggregates. Hence it has two components, as shown in Fig. 5(b), which is fitted to Eq. (8) yielding the ratio, $S_{0,\mathrm{aggregate}}/S_{0,\mathrm{monomer}} = 1.5$ which reports on the fractions of aggregate and monomer in solution.

Finally, it is possible for the monomer and aggregate to have different relaxation rates [27]. In this case, for the pulsed-field gradient stimulated echo (Fig. 1), we can have a more complicated signal attenuation expression,

$$S_{\mathrm{total}} = \sum_i S_i \exp(-R_{1,i}\tau_1)\exp(-2R_{2,i}\tau_2)\exp(-D_i k(\Delta)), \tag{10}$$

where $R_{1,i}$ and $R_{2,i}$ are the effective longitudinal and transverse relaxation rates of the ith species. Given that τ_2 is not varied, and $\tau_2 \ll \tau_1 \sim \Delta$, one can write this approximately as

$$S_{\mathrm{total}} = \sum_i S_i \exp(-R_{1,i}\Delta)\exp(-D_i k(\Delta)). \tag{11}$$

Once again, in the event that the argument of the diffusion exponentials is small, this can be approximated as $S_{\mathrm{total}}/S_{\max} = \exp(-D_{\mathrm{Obs}}k)$. In this case, one observes mono-exponential behaviour, but the

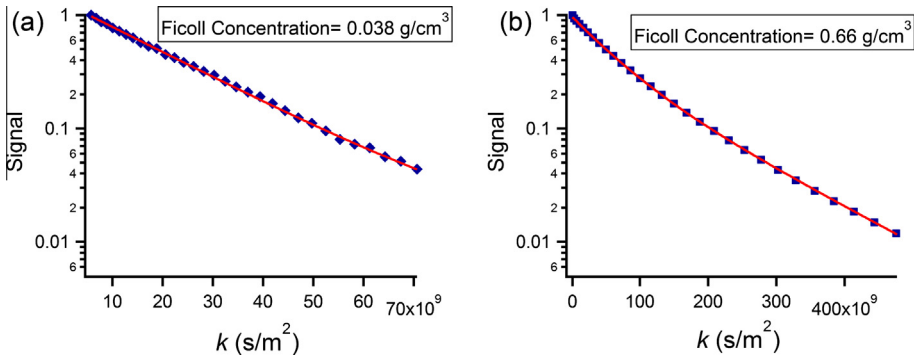

Fig. 5. The attenuation of the signal $S(k)/S(0)$ on a log scale versus the gradient strength parameter $k = (\gamma\delta g)^2\ (\Delta - \delta/3)$ for an aqueous solution of the polysaccharide Ficoll-70 (a) is monoexponential at low concentration (b) is biexponential at high concentration. Gradient pulse duration $\delta = 2$ ms and the diffusion time $\Delta = 500$ ms.

observed diffusion coefficient is relaxation weighted; when there are just two species, i.e. monomer and aggregate, one gets

$$D_{\mathrm{Obs}} = \frac{f\exp(-R_{1,1}\Delta)D_1 + (1-f)\exp(-R_{1,2}\Delta)D_2}{f\exp(-R_{1,1}\Delta) + (1-f)\exp(-R_{1,2}\Delta)}, \qquad (12)$$

where $R_{1,1}$ and $R_{1,2}$ are the effective longitudinal relaxation rates for components 1 (monomer) and 2 (aggregate), and f and $1-f$ are the fractions in the monomeric and aggregate states. The relaxation weighting in Eq. (12), reported by Price and coworkers [47], has an interesting consequence: if the effective relaxation rate ($R_{1,2}$) associated with an aggregate is significantly larger than that associated with the monomer ($R_{1,1}$), then the weight corresponding to the aggregate diffusion will decrease with time, and since $D_1 > D_2$, the observed diffusion coefficient will increase as a function of Δ. In concentrated lysozyme solutions, it was possible to use this phenomenon to resolve a disagreement between two small-angle scattering experiments [48], and to confirm and quantify the existence of lysozyme clusters in equilibrium [49]. Interestingly, this finding was in agreement with results from q-resolved diffusion measurements obtained *via* the neutron spin echo technique [50]. Whereas the cluster peak in small-angle scattering must be careful distinguished from possible low-Q artifacts, the clusters in PFG-NMR have a distinct chemical- shift signature.

We end this section with a caution and an advertisement. Measured diffusion coefficients are often not the bare dynamical quantities of interest. Careful measurements as a function of some variable parameter – in Section 3 the total surfactant concentration – are often required to obtain the true monomer and aggregate diffusion coefficients. In addition, one can also obtain the *composition*: that is, the fractions of aggregate and monomer. Curiously, with multiple species with distinct chemical shift signatures, PFG-NMR actually gives more information in the two-component polymer–surfactant complex (Fig. 3(a)) than in the pure-surfactant system (Fig. 4), because one has separate equations for each species. This contrasts with scattering-based techniques, where the presence of multiple components *always* makes interpretation harder. PFG-NMR is thus a unique dynamical modality for probing multi-component macromolecular solutions.

5. Complex formation in a peptide–surfactant system

Excluded volume "obstruction" effects must clearly affect the dynamics of proteins, peptides and amino acids in crowded environments. In addition, the dynamics can also be affected by electrostatic interactions between macromolecules, as well as complex formation. All these effects are likely to be sensitive to the electrostatic environment. Virk et al. [51] examined the dynamics of four amino acids using PFG-NMR experiments (Fig. 6), and coupled this with molecular dynamics (MD) simulations via models that incorporate obstruction (excluded volume effects) and complex formation. The MD simulations are quite sensitive to the force field used; nevertheless Virk et al. find strong evidence for the importance of obstruction effects, but also find that complex formation is likely to be relevant because all experimental diffusion coefficients are lower than those predicted by obstruction-only models. However, scaling their experimental diffusion coefficients with respect to those at zero concentration for all four amino acids, and plotting against the volume fraction, one finds that their data for all 4 amino acids collapse, more or less, onto one curve, providing strong experimental evidence that any complex formation that occurs is also tied to excluded volume effects.

Barhoum et al. [30] used PFG-NMR to study diffusion in peptide–micelle complexes in a system consisting of antimicrobial peptide (GAD-2, which has a 19-amino acid sequence [52–54]) and anionic surfactant SDS, where electrostatic interactions are likely to be important. Antimicrobial peptides (AMPs) contain 12–50 amino acids. Interactions between the anionic residues of the AMPs and anionic micelles such as SDS have been commonly used to provide a membrane-mimic environment in structural studies of membrane proteins and AMPs [55–63].

The 1D proton NMR spectrum consists of peak regions corresponding to HDO, peptide (GAD-2), and SDS. Each species has peaks that are spectrally distinct, and the signal attenuations associated with GAD-2 and SDS are monoexponential. The CAC in this system is ≈1 mM, and therefore residence times of SDS within

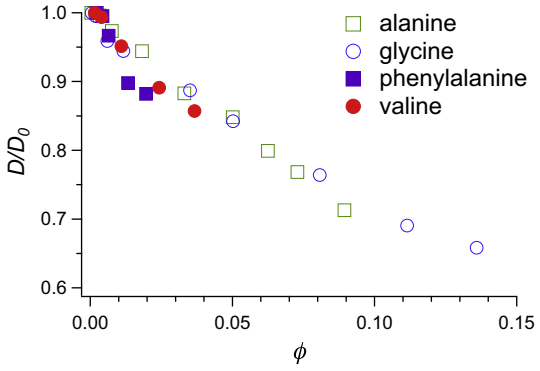

Fig. 6. Scaled diffusion coefficients for amino acids alanine, glycine, phenylalanine and valine, plotted against volume fraction up to their solubility limit, nearly collapse onto one universal curve. The experimental diffusion coefficients are lower than those predicted by obstruction-only models. Data adapted from figure originally published in Amninder S. Virk et al. (2015) Macromolecular crowding studies of amino acids using NMR diffusion measurements and molecular dynamics simulations, Front. Phys., 02 February, 2015 [51].

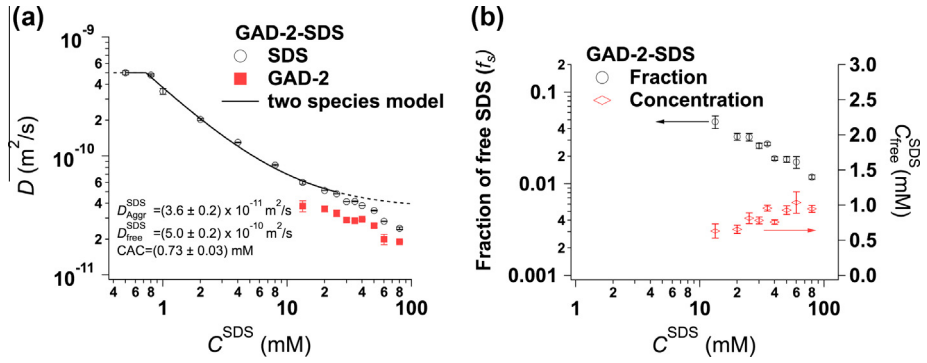

Fig. 7. (a) Self-diffusion coefficient of GAD-2 and SDS in a GAD-2-SDS system with R = [SDS]/[GAD-2] = 30 versus SDS concentration C^{SDS}. (b) Fraction (f_s) of free SDS and concentration $\left(C_{free}^{SDS}\right)$ of free SDS versus SDS concentration C^{SDS}. Reproduced with permission from Suliman Barhoum, Valerie Booth, and Anand Yethiraj. Eur Biophys J. 2013, 42(5):405–14.

the complex are only slightly longer than in the PEO-SDS system. This suggests that the SDS visits more than one environment over very short timescales, and Eqs. (5) and (7) apply. Similar phenomena were also observed in previous studies [41–43]. The observed self-diffusion coefficient is thus a weighted average of SDS in monomer form and SDS in a micellar or GAD-2-SDS aggregate. A simplifying factor in associating macromolecular solutions is that the concentration of SDS is 30 times higher than the GAD-2 concentration, and one can thus assume there is no free peptide. This is generally true for peptide and protein solutions where the peptide/protein concentrations are usually low.

The SDS self-diffusion coefficient could be fitted to the two-site rapid exchange model of Eq. (5) in the SDS concentration regime below 25 mM (Fig. 7(a), solid line) but deviates from this model at higher SDS concentrations. This is broadly consistent with the behaviours in polymer–surfactant solutions, and yields $D_{free}^{SDS} = (5.0 \pm 0.2) \times 10^{-10}$ m^2/s, $D_{Aggr}^{SDS} = (3.6 \pm 0.2) \times 10^{-11}$ m^2/s, and CAC = (0.73 ± 0.03) mM. The fraction (f_s) and the concentration of free SDS $\left(C_{free}^{SDS}\right)$ for the GAD-2-SDS system over the whole range of SDS concentration was calculated using the two-site exchange model (Eq. (5)) with $D_{Aggr}^{SDS} = D^{Peptide}$ (Fig. 7(b)).

$$f_s = \frac{C_{free}^{SDS}}{C^{SDS}} = \frac{D_{Obs}^{SDS} - D^{Peptide}}{D_{free}^{SDS} - D^{Peptide}}. \quad (13)$$

The fraction f_s of free SDS decreases with increasing SDS concentration (C^{SDS}). Also, the concentration of free SDS $\left(C_{free}^{SDS}\right)$ increases from approximately the CAC = 0.7 mM to approximately the CMC = 1 mM (Fig. 3(a)). This agrees, once again, with the expectation that the concentration of free surfactant should not exceed the CMC [29,45,46].

PFG-NMR study of the dynamics of peptide–surfactant complexes addresses a practical problem of relevance to biochemists and biophysicists. It provides quantitatively the SDS concentration regime where the two-species model is unambiguously valid. This regime was identified to be below C^{SDS} of 25 mM, where macromolecular crowding does not take place. Thus, all measurements geared at measuring the sizes of complexes (whether PFG NMR, DLS or SANS!) should be done in this low-concentration regime.

6. Confinement-influenced diffusion in wormlike micelles

Finally, we discuss the effects of *confinement* on diffusion measurements in complex-forming systems [31,64,65]. As an example along similar lines to the previous ones, we consider a complex between the anionic SDS and another macromolecule, this time the zwitterionic surfactant N-tetradecyl-N,N-dimethyl-3-ammonio-1-propanesulfonate ("TDPS") in a salt-rich aqueous solution. This system was studied extensively by rheology and scattering by Castillo and coworkers [66–68], but microscopic dynamics *within* a cylindrical/wormlike micelle were not accessible to these techniques.

Important aspects of this system are different to those discussed earlier. First, the TDPS and SDS peaks are not separable by chemical shift, so independent information on the two components cannot be obtained, as was possible in the previous examples. Second, both macromolecular components are charged surfactants of roughly the same size. Third, both surfactants are present in reasonably high concentrations. In addition, because TDPS is zwitterionic, there is likely to be strong association, driven by electrostatic interactions, between the two surfactants, and one expects a composite TDPS-SDS aggregate. Previous work indicated that the microscopic structures were wormlike micelles, and thus this system was treated far more like a single component system. In such a case, it is necessary to couple PFG ^{1}H NMR with other modalities. Barhoum et al. used relaxation, ^{2}H (deuterium) NMR, and rheometry in addition to PFG-NMR to study the TDPS-SDS wormlike micellar system [69].

The variation of longitudinal relaxation rates as a function of the concentration C_z of the zwitterionic surfactant TDPS shows an exponential saturation: the exponent of this saturation is ~5 mM, consistent with the overlap concentration $C^\star$ identified by Castillo and coworkers [67]. Next, the diffusion coefficient was obtained from a single-exponential fit of the signal attenuation, for different diffusion times Δ. The observed surfactant diffusion coefficient decreased with Δ (Fig. 8(a)). Since the critical aggregation concentration for this system is approximately 1 order of magnitude lower than in the PEO-SDS system, the residence time of the surfactant molecule within the aggregate is correspondingly longer, and at high surfactant concentrations, practically all the surfactant is within the micelle. This suggests that the decrease arises from the fact that the longer the time for which a molecule diffuses, the more likely it is to experience the confining boundaries of the micelle, which is visualized as a long, 1-dimensional cylindrical cavity.

One can plot the apparent mean-square displacement (MSD) as a function of the diffusion time Δ, using $\langle z^2 \rangle = 2D_{Obs}\Delta$. While the behaviour is linear for times longer than 50 ms, the extrapolation to zero Δ leads to a non-zero MSD, consistent with fast molecular diffusion at short times (too short to access on the NMR timescale) and slower micellar diffusion at longer times. Fig. 8(c) shows a plot of $\ln(D_m)$ versus the scaled zwitterionic surfactant concentration $\ln(C_z/C^\star)$, in the semi-dilute regime, measured along the x, y, and z directions: the x and y components are shifted downwards, for better visualization, because all three datasets overlap perfectly. A

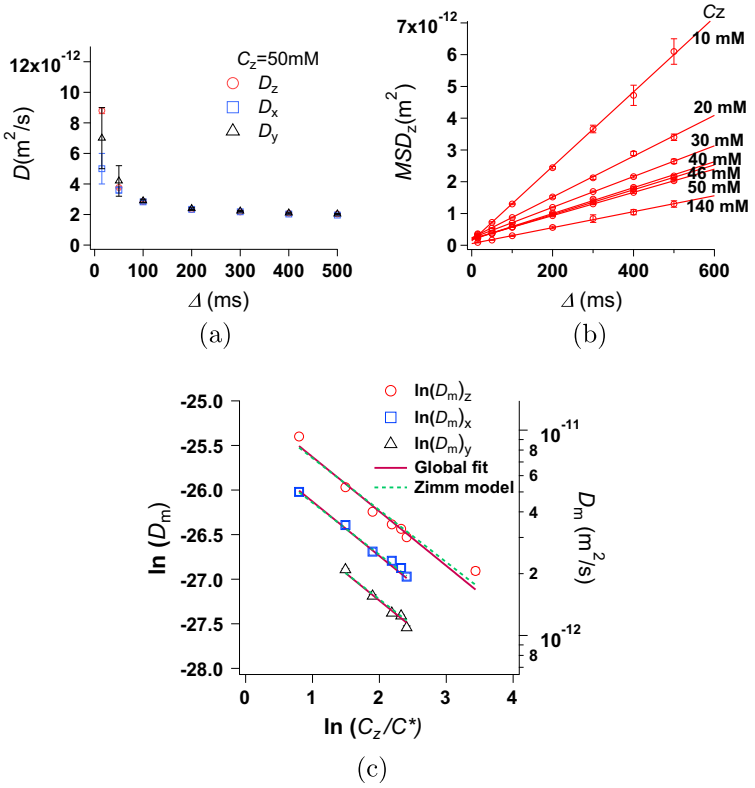

Fig. 8. (a) TDPS-SDS self-diffusion coefficient (D_x, D_y, D_z) versus diffusion time Δ. $C_z = 50$ mM. (b) Z-axis mean square displacement MSD_z versus diffusion time Δ. The intercepts are not zero but on the 0.5 μm scale. (c) Anisotropic micelle self-diffusion coefficients $(D_{m,z}, D_{m,x}, D_{m,y})$ extracted from the slopes of the mean-square displacement MSD curves as a function of TDPS concentration (C_z) for TDPS/SDS/NaCl(0.5M)/D_2O samples at $T = 298$ K. Measurements along x and y are shifted vertically for clarity, as all data sets overlap. Reproduced from S. Barhoum, R. Castillo, A. Yethiraj. Characterization of dynamics and internal structure of a mixed-surfactant wormlike micellar system using NMR and rheometry. Soft Matter, 2012, 8, 29502957 [69].

simultaneous fit to all 3 datasets yields a power law $D = D_Z\left(C/C^{\star}\right)^{-d}$ with the exponent $d = -0.58 \pm 0.03$. The Zimm model for polymer dynamics in a good solvent, which considers the hydrodynamic interactions between the monomers in the polymer chain and between the monomers and the solvent molecules, predicts an exponent $d = (1-\nu)/(3\nu-1) = 0.54$ (using $\nu = 0.588$ for a self-avoiding polymer) [70]. This exponent is shown for comparison (dashed line labelled "Zimm model" in the graph). We calculate an experimental exponent $\nu = (1+d)/(1+3d) = 0.58 \pm 0.01$. From the power law fit, we also obtain an average Zimm diffusion coefficient D_Z for the wormlike micelle of $8.3(1)\times 10^{-12}$ m^2/s.

In the presence of cylindrical confinement, one can directly fit the signal attenuation to the form for diffusion in a cylindrical cavity [23]:

$$\ln[S(q)] = -((2\pi q)^2)D_m\Delta + \ln\left[\frac{2[1-\cos(2\pi qL_z)]}{(2\pi qL_z)^2} + 4(2\pi qL_z)^2\sum_{n=1}^{N}\exp\left(-\frac{n^2\pi^2 D_s\Delta}{L_z^2}\right)\times\frac{1-(-1)^n\cos(2\pi qL_z)}{\left((2\pi qL_z)^2-(n\pi)^2\right)^2}\right]. \quad (14)$$

Here D_s is the molecular bulk surfactant self-diffusion, D_m is the micellar self-diffusion, $q = \gamma\delta g/(2\pi)$ and L_z is the average length of a one-dimensional channel. The infinite sum in Eq. (14) was adequately approximated in [69] by an upper limit $N = 1000$. While this equation looks complicated, it has only one free parameter, L_z, because the surfactant diffusion coefficient D_s is known, and we can use the micellar diffusion coefficient D_m obtained from Fig. 8(c). Quite remarkably, all the signal attenuations could be fitted using the C_z-dependent micellar diffusion coefficient obtained in Fig. 8(b), using one surfactant diffusion coefficient $(D_s = 13\times 10^{-12}$ m^2/s) and to a single wormlike micelle length $L_z \approx 1$ μm.

This is another example where one can get system-specific structural $(L_z \approx 1$ μm) and dynamical $(D_Z = 8.3(1)\times 10^{-12}$ m^2/s) information from PFG-NMR experiments.

7. Summary

Pulsed-field gradient NMR provides a unique window through which to study the dynamics of many systems where macromolecular crowding is important. The fact that different species give signals at different chemical shifts allows simultaneous measurement of their individual dynamics. At the same time, in the presence of complex formation, multiple associated species move together. It was shown in this review that this constraint, coupled with the chemical shift signatures, allows PFG-NMR to yield new informations in old systems. Experiments are currently under way in our group to couple PFG-NMR with a direct structural probe such as SANS. It is expected that the tandem use of these two powerful experimental modalities will yield new insights, and allow unambiguous determination, in model crowded systems, of the hydrodynamic function defined in Eq. (3).

The dynamics of a variety of macromolecular systems have been presented in this review: pure surfactants, mixed surfactants, polymer–surfactant complexes, peptides, and peptide–surfactant complexes. These systems exhibit aspects that are important in biology: diffusion in the presence of inter-macromolecular interactions, arising from steric excluded volume effects, electrostatic interactions (*via* the buffer) and/or long-range hydrodynamic interactions, and dynamics in the presence of confinement.

The dominant conclusion of the PFG-NMR diffusometry exploration in complex-forming systems is that an uncritical use of Eq. (1) to extract hydrodynamic radii can yield (and has yielded) incorrect results. First, the character of the signal attenuations must be determined: are they mono-exponential or not? Then, if mono-exponential, a model (in our example, Eq. (5)) must be employed to interpret the observed diffusion coefficients. We have seen that there is usually enough information in the NMR measurements to check for self-consistency of the model.

In the single-surfactant studies, there is only one component (SDS), and the system is not at high packing fraction. The onset of crowding in this system, at a surfactant concentration of ~60 mM (packing fraction $\phi < 0.1$), is governed by hydrodynamics in a system where electrostatics is very important. In the aqueous system of small peptides, complex formation is likely to be important but the details of the peptide do not seem to affect the dynamics significantly.

In the polymer–surfactant solution (PEO-SDS), this onset is signalled by the surfactant monomer concentration increasing above the CAC and reaching the CMC, and the prevalence of three species (surfactant monomer, polymer–surfactant aggregate and free surfactant micelle). This onset also applies to the peptide–surfactant system (GAD-2-SDS). The peptide GAD-2 was shown to form complexes with surfactant micelles for which the complex size is dependent on concentration even in the regime prior to the onset of crowding.

In the two-surfactant TDPS-SDS system, PFG-NMR measurements report on surfactant diffusion within a confined cylindrical micelle at short times, and on micellar diffusion at long times. The micellar diffusion was in remarkable agreement with concentration-dependent scaling predictions based on the Zimm model.

In summary, it is hoped that this review will encourage broader use of the PFG-NMR technique to study macromolecular dynamics in soft and bio-materials.

Acknowledgement

This work was funded by the Natural Sciences and Engineering Research Council of Canada. We thank Bill Price for providing us with the data used to plot Fig. 6.

References

[1] A.B. Fulton, How crowded is the cytoplasm?, Cell 30 (1982) 345
[2] S.B. Zimmerman, A.P. Minton, Macromolecular crowding: biochemical, biophysical, and physiological consequences, Annu. Rev. Biophys. Biomol. Struct. 22 (1993) 27.
[3] R.J. Ellis, Macromolecular crowding: obvious but underappreciated, Trends Biochem. Sci. 26 (2001) 597–604.
[4] C. Li, Y. Wang, G.J. Pielak, Translational and rotational diffusion of a small globular protein under crowded conditions, J. Phys. Chem. B 113 (2009) 13390–13392.
[5] I. Pastor, E. Vilaseca, S. Madurga, J.L. Garces, M. Cascante, F. Mas, Diffusion of r-chymotrypsin in solution-crowded media. A fluorescence recovery after photobleaching study, J. Phys. Chem. B 114 (2010) 4028–4034.
[6] S. Zorrilla, M.A. Hink, A.J.W.G. Visser, M.P. Lillo, Translational and rotational motions of proteins in a protein crowded environment, Biophys. Chem. 125 (2007) 298–305.
[7] D. Hall, M. Hoshino, Effects of macromolecular crowding on intracellular diffusion from a single particle perspective, Biophys. Rev. 2 (2010) 39–53.
[8] Y. Wang, C. Li, G.J. Pielak, Effects of proteins on protein diffusion, J. Am. Chem. Soc. 132 (2010) 9392–9397.
[9] P. Bernado, J.G. de la Torre, M. Pons, in biological systems: hydrodynamics and NMR methods, J. Mol. Recognit. 17 (2004) 397–407.
[10] J.A. Dix, A. Verkman, Crowding effects on diffusion in solutions and cells, Ann. Rev. Biophys. 37 (2008) 247–263.
[11] H.X. Zhou, G. Rivas, A.P. Minton, Macromolecular crowding and confinement: biochemical, biophysical, and potential physiological consequences, Ann. Rev. Biophys. 37 (2008) 375–397.
[12] Y. Wang, M. Sarkar, A.E. Smith, A.S. Krois, G.J. Pielak, Macromolecular crowding and protein stability, J. Am. Chem. Soc. 134 (2012) 16614–16618.
[13] M. Muschol, F. Rosenberger, Interactions in undersaturated and supersaturated lysozyme solutions: static and dynamic light scattering results, J. Chem. Phys. 103 (1995) 10424.
[14] S.B. Zimmerman, A.P. Minton, Macromolecular crowding: biochemical, biophysical, and physiological consequences, Annu. Rev. Biophys. Biomol. Struct. 22 (1993) 27–65.
[15] B.-R. Zhou, Y. Liang, F. Du, Z. Zhou, J. Chen, Mixed macromolecular crowding accelerates the oxidative refolding of reduced, denatured lysozyme, J. Biol. Chem. 279 (2004) 55109–55116.
[16] B.-R. Zhou, Z. Zhou, Q.-L. Hu, J. Chen, Y. Liang, Mixed macromolecular crowding inhibits amyloid formation of hen egg white lysozyme, Biochim. Biophys. Acta 1784 (2008) 472–480.
[17] G.K. Batchelor, Sedimentation in a dilute dispersion of spheres, J. Fluid Mech. 52 (1972) 245.
[18] W.B. Russel, D.A. Saville, W.R. Schowalter, Colloidal Dispersions, Cambridge University Press, England, 1989.
[19] W. Härtl, J. Wagner, C. Beck, F. Gierschner, R. Hempelmann, Self-diffusion and hydrodynamic interactions in highly charged colloids, J. Phys.: Condens. Matter 12 (8A) (2000) A287.
[20] A.J. Banchio, J. Gapinski, A. Patkowski, W. Häußler, A. Fluerasu, S. Sacanna, P. Holmqvist, G. Meier, M.P. Lettinga, G. Nägele, Many-body hydrodynamic interactions in charge-stabilized suspensions, Phys. Rev. Lett. 96 (2006) 138303.
[21] B.J. Berne, R. Pecora, Dynamic Light Scattering: With Applications to Chemistry, Biology, and Physics, Dover Publications, Mineola, NY, 2000.
[22] P. Lindner, T. Zemb (Eds.), Neutrons, X-rays, and Light: Scattering Methods Applied to Soft Condensed Matter, first ed., North-Holland Delta Series, Elsevier, Amsterdam: Boston, 2002.
[23] P.T. Callaghan, Principles of Nuclear Magnetic Resonance Microscopy, Oxford Science Publications, London, 1991.
[24] W.S. Price, NMR Studies of Translational Motion: Principles and Applications, first ed., Cambridge University Press, Cambridge, UK, 2009.
[25] G.A. Morris, Diffusion-ordered spectroscopy, in: R.K. Harris (Ed.), Encyclopedia of Magnetic Resonance, John Wiley & Sons, Ltd, Chichester, UK, 2009.
[26] K.I. Momot, P.W. Kuchel, PFG NMR diffusion experiments for complex systems, Conc. Magn. Reson. Part A 28A (2006) 249.
[27] T. Stait-Gardner, S.A. Willis, N.N. Yadav, G. Zheng, W.S. Price, NMR diffusion measurements of complex systems, Diffus. Fund. 11 (2009) 15.
[28] O. Söderman, P. Stilbs, Nmr studies of complex surfactant systems, Prog. Nucl. Magn. Reson. Spectrosc. 26 (1994) 445.
[29] S. Barhoum, A. Yethiraj, An NMR study of macromolecular aggregation in a model polymer–surfactant solution, J. Chem. Phys. 132 (2010) 024909.
[30] S. Barhoum, V. Booth, A. Yethiraj, Diffusion NMR study of complex formation in membrane-associated peptides, Eur. Biophys. J. 42 (2013) 405–414.
[31] W.S. Price, Pulsed-field gradient nuclear magnetic resonance as a tool for studying translational diffusion: Part I. Basic theory, Conc. Magn. Reson. 9 (1997) 299–336.
[32] K. Chari, B. Antalek, J. Minter, Diffusion and scaling behavior of polymer–surfactant aggregates, Phys. Rev. Lett. 74 (1995) 3624–3627.
[33] H. Yuan, L. Luo, L. Zhang, S. Zhao, S. Mao, J. Yu, L. Shen, Y. Du, Aggregation of sodium dodecyl sulfate in poly(ethylene glycol) aqueous solution studied by ^{1}H NMR spectroscopy, Colloid Polym. Sci. 280 (2002) 479–484.
[34] F. Asora, L. Feruglio, G. Pellizer, ^{23}Na relaxation in SDS and SDES-polymer systems, Colloids Surfaces A: Physicochem. Eng. Aspects 245 (2004) 127–132.
[35] M.I. Gjerde, W. Nerdal, H. Hoiland, Interactions between poly(ethylene oxide) and sodium dodecyl sulfate as studied by NMR, conductivity, and viscosity at 283.1–298.1 K, J. Colloid Interf. Sci. 197 (1998) 191–197.
[36] J. Francois, J. Dayantis, J. Sabbadin, Hydrodynamical behaviour of the poly (ethylene oxide)-sodium dodecylsulphate complex, Eur. Polym. J. 21 (1985) 165–174.
[37] E. Minatti, D. Zanette, Salt effects on the interaction of poly(ethylene oxide) and sodium dodecyl sulfate measured by conductivity, Colloids Surf. A 113 (1996) 237–246.
[38] E. Pettersson, D. Topgaard, P. Stilbs, O. Söderman, Surfactant/nonionic polymer interaction. A NMR diffusometry and NMR electrophoretic investigation, Langmuir 20 (2004) 1138–1143.
[39] H. Evertsson, S. Nilsson, C.J. Welch, L.-O. Sundelof, Molecular dynamics in dilute aqueous solutions of ethyl(hydroxyethyl)cellulose and sodium dodecyl sulfate as investigated by proton NMR relaxation, Langmuir 14 (1998) 6403–6408.
[40] B. Cabane, R. Duplessix, Organization of surfactant micelles adsorbed on a polymer molecule in water: a neutron scattering study, J. Phys. 43 (1982) 1529–1542.
[41] O. Söderman, P. Stilbs, NMR studies of complex surfactant systems, Prog. Nucl. Magn. Reson. Spectrosc. 26 (1994) 445–482.
[42] P. Stilbs, Fourier transform NMR pulsed-gradient spin-echo (FT-PFGSE) self diffusion measurements of solubilization equilibria in sds solutions, J. Colloid Interf. Sci. 87 (1982) 385–394.
[43] P. Stilbs, A comparative study of micellar solubilization for combinations of surfactants and solubilizates using the fourier transform pulsed-gradient spin-echo NMR multicomponent self-diffusion technique, J. Colloid Interf. Sci. 94 (1983) 463–469.
[44] T. Ando, J. Skolnick, Crowding and hydrodynamic interactions likely dominate in vivo macromolecular motion, PNAS 107 (2010) 18457–18462.
[45] J.N. Israelachvili, Intermolecular and Surface Forces, third ed., Academic Press, Burlington, MA, 2011.

[46] R.A.L. Jones, Soft Condensed Matter, first ed., Oxford University Press Inc, New York, 2002.
[47] W.S. Price, F. Tsuchiya, Y. Arata, Time dependence of aggregation in crystallizing lysozyme solutions probed using NMR self-diffusion measurements, Biophys. J. 80 (2001) 1585–1590.
[48] J. Trewhella, The different views from small angles, Proc. Nat. Acad. Sci. 105 (13) (2008) 4967–4968.
[49] S. Barhoum, A. Yethiraj, NMR detection of an equilibrium phase consisting of monomers and clusters in concentrated lysozyme solutions, J. Phys. Chem. B 114 (2010) 17062–17067.
[50] L. Porcar, P. Falus, W.-R. Chen, A. Faraone, E. Fratini, K. Hong, P. Baglioni, Y. Liu, Formation of the dynamic clusters in concentrated lysozyme protein solutions, J. Phys. Chem. Lett. 1 (2010) 126–129.
[51] A.S. Virk, T. Stait-Gardner, S.A. Willis, A.M. Torres, W.S. Price, Macromolecular crowding studies of amino acids using NMR diffusion measurements and molecular dynamics simulations, Front. Phys. 3 (2015) 1–15.
[52] J.M.O. Fernandes, J. Ruangsri, V. Kiron, Atlantic cod piscidin and its diversification through positive selection, Public Libr. Sci. 5 (2010) 1–7.
[53] M.J. Browne, C.Y. Feng, V. Booth, M.L. Rise, Characterization and expression studies of gaduscidin-1 and gaduscidin-2; paralogous antimicrobial peptide-like transcripts from atlantic cod (gadus morhua), Dev. Comp. Immunol. 35 (2011) 399–408.
[54] J. Ruangsri, S.A. Salger, C.M. Caipang, V. Kiron, J.M. Fernandes, Differential expression and biological activity of two piscidin paralogues and a novel splice variant in atlantic cod (gadus morhua l.), Fish Shellfish Immunol. 32 (2012) 396–406.
[55] G. Wang, NMR studies of a model antimicrobial peptide in the micelles of SDS, dodecylphosphocholine, or dioctanoylphosphatidylglycerol, Open Magn. Reson. J. 1 (2008) 9–15.
[56] G. Wang, Structural biology of antimicrobial peptides by NMR spectroscopy, Curr. Org. Chem. 10 (1999) 569–581.
[57] T.L. Whitehead, L.M. Jones, R.P. Hicks, Effects of the incorporation of CHAPS into SDS micelles on neuropeptide–micelle binding: separation of the role of electrostatic interactions from hydrophobic interactions, Biopolymers 58 (2001) 593–605.
[58] L. Orfi, M. Lin, C.K. Larive, Measurement of SDS micelle-peptide association using ^{1}H NMR chemical shift analysis and pulsed-field gradient NMR spectroscopy, J. Anal. Chem. 70 (1998) 1339–1345.
[59] B.A. Begotka, J.L. Hunsader, C. Oparaeche, J.K. Vincent, K.F. Morris, A pulsed field gradient NMR diffusion investigation of enkephalin peptide-sodium dodecyl sulfate micelle association, Magn. Reson. Chem. 44 (2006) 586–593.
[60] K.R. Deaton, E.A. Feyen, H.J. Nkulabi, K.F. Morris, Pulsed-field gradient NMR study of sodium dodecyl sulfate micelle-peptide association, Magn. Reson. Chem. 39 (2001) 276–282.
[61] T.L. Whitehead, L.M. Jones, R.P. Hicks, PFG-NMR investigations of the binding of cationic neuropeptides to anionic and zwitterionic micelles, J. Biomol. Struct. Dyn. 21 (2004) 567–576.
[62] X. Gao, T.C. Wong, Studies of the binding and structure of adrenocorticotropin peptides in membrane mimics by NMR spectroscopy and pulsed-field gradient diffusion, Biophys. J . 75 (1998) 1871–1888.
[63] G.W. Buchko, A. Rozek, D.W. Hoyt, R.J. Cushley, M.A. Kennedy, The use of sodium dodecyl sulfate to model the apolipoprotein environment. evidence for peptide SDS complexes using pulsed-field-gradient NMR spectroscopy, Biochim. Biophys. Acta 1392 (1998) 101–108.
[64] P.T. Callaghan, Pulsed gradient spin echo NMR for planar, cylindrical and spherical pores under conditions of wall relaxation, J. Magn. Reson. A113 (1995) 53–59.
[65] P.T. Callaghan, A. Coy, PGSE NMR and molecular translational motion in porous media, in: P. Tycko (Ed.), NMR Probes and Molecular Dynamics, Kluwer Academic, Dordrecht, The Netherlands, 1994.
[66] D. Lopez-Diaz, R. Castillo, The wormlike micellar solution made of a zwitterionic surfactant (TDPS), an anionic surfactant (SDS), and brine in the semidilute regime, J. Phys. Chem. B 114 (2010) 8917–8925.
[67] D. Lopez-Diaz, E. Sarmiento-Gomez, C. Garza, R. Castillo, A rheological study in the dilute regime of the worm-micelle fluid made of zwitterionic surfactant (TDPS), anionic surfactant (SDS), and brine, J. Colloid Interf. Sci. 348 (2010) 152–158.
[68] E. Sarmiento-Gomez, D. Lopez-Diaz, R. Castillo, Microrheology and characteristic lengths in wormlike micelles made of a zwitterionic surfactant and sds in brine, J. Phys. Chem. B 114 (2010) 12193–12202.
[69] S. Barhoum, R. Castillo, A. Yethiraj, Characterization of dynamics and internal structure of a mixed-surfactant wormlike micellar system using nmr and rheometry, Soft Matter 8 (2012) 6950–6957.
[70] M. Rubinstein, R.H. Colby, Polymer Physics, first ed., Oxford University Press, New York, 2003.

Glossary of abbreviations

PEG: Polyethylene glycol
BSA: Bovine serum albumin
DLS: Dynamic light scattering
FCS: Fluorescence correlation spectroscopy
SAXS: Small-angle X-ray scattering
SANS: Small-angle neutron scattering
PFG-NMR: Pulsed-field gradient NMR
DOSY: Diffusion-ordered spectroscopy
AMP: Antimicrobial peptide
SDS: Sodium dodecylsulphate
GAD-2: Gaduscidin-2
PEO: Polyethylene oxide
TDPS: N-tetradecyl N,N-dimethyl-3-ammonio-1-propanesulfonate
CAC: Critical aggregation concentration
CMC: Critical micellar concentration
MD: Molecular dynamics
MSD: Mean square displacement